ResearchGate

See discussions, stats, and author profiles for this publication at: https://www.researchgate.net/publication/216517836

Electrodeposition of ZnO Nanostructures on Molecular Thin Films

ARTICLE *in* CHEMISTRY OF MATERIALS · SEPTEMBER 2011

Impact Factor: 8.35 · DOI: 10.1021/cm200764h

CITATIONS
27

READS
61

11 AUTHORS, INCLUDING:

Benoit Illy
Imperial College London
15 PUBLICATIONS **384** CITATIONS
SEE PROFILE

Tim S. Jones
The University of Warwick
324 PUBLICATIONS **6,704** CITATIONS
SEE PROFILE

Sandrine Heutz
Imperial College London
62 PUBLICATIONS **1,266** CITATIONS
SEE PROFILE

Martyn Mclachlan
Imperial College London
53 PUBLICATIONS **543** CITATIONS
SEE PROFILE

Available from: Benoit Illy
Retrieved on: 29 January 2016

CHEMISTRY OF MATERIALS

ARTICLE

pubs.acs.org/cm

Electrodeposition of ZnO Nanostructures on Molecular Thin Films

Amy C. Cruickshank,[†] Stephen E. R. Tay,[†,‡] Benoit N. Illy,[†] Raffaello Da Campo,[§] Stefan Schumann,[§] Tim S. Jones,[§] Sandrine Heutz,[†] Martyn A. McLachlan,[†] David W. McComb,[†] D. Jason Riley,[†] and Mary P. Ryan*[,†]

[†]Department of Materials and London Centre for Nanotechnology, Imperial College London, Exhibition Road, London SW7 2AZ, United Kingdom

[‡]School of Materials Science and Engineering, Nanyang Technological University, Nanyang Avenue, Singapore 639798

[§]Department of Chemistry, University of Warwick, Coventry CV4 7AL, United Kingdom

Supporting Information

ABSTRACT: Electrodeposition of highly crystalline ZnO nanostructures *directly* onto copper phthalocyanine and pentacene thin films, from aqueous solutions containing zinc nitrate and dissolved oxygen, has been successfully demonstrated for the first time using a two-step electrochemical deposition process. Importantly, surface activation of the molecular thin film substrates by depositing a thin layer of ZnO nanoparticles at high cathodic overpotentials prior to film growth was found to be *crucial* for achieving a dense coverage of ZnO nanostructures with uniform morphology. The mechanism for ZnO deposition via electroreduction of hydroxide precursor species (oxygen and NO_3^- ions) at the organic-electrolyte interface was shown to be analogous to that reported for conventional inorganic and metal electrodes. Comparison of cathodic current density-time curves, measured during deposition, with film orientation and morphology revealed that the cathodic current density and number of nucleation sites are key factors in determining the characteristics of ZnO film growth on organic substrates. Significantly, the CuPc and pentacene films are not damaged or degraded during this process.

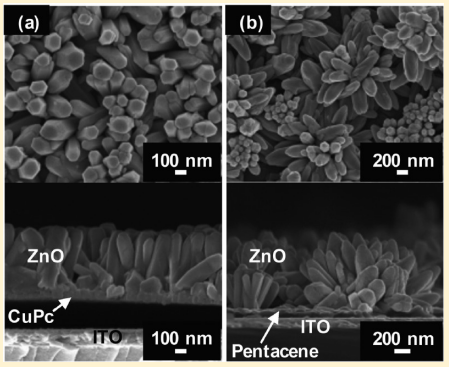

KEYWORDS: ZnO, electrodeposition, molecular thin films, copper phthalocyanine, pentacene

1. INTRODUCTION

Hybrid ZnO-organic thin film structures have attracted increasing research attention for incorporation into low-cost electronic and photonic devices such as sensors,[1] solar cells,[2−5] and light-emitting diodes.[6−8] These materials combine the high flexibility of conjugated small molecules or polymers with the structural and chemical stability of inorganic materials and therefore, promise new properties that are superior to those available in a single class of materials. Furthermore, the ability to nanostructure hybrid materials to maximize interfacial areas and tailor the dimensions of the inorganic phase to the properties of the organic materials has been found to dramatically improve charge transport processes[9] and enhance optoelectronic properties.[10]

A variety of methods have been established for ZnO film preparation such as molecular beam epitaxy,[11] RF magnetron sputtering,[12] pulsed laser deposition,[13] spray pyrolysis,[2] chemical bath deposition,[14] and electrodeposition.[15,16] For ease of processing, hybrid ZnO-organic thin film devices are often prepared by fabricating the organic phase on top of the ZnO layer to avoid processing damage to the soft organic films. In many industrial processes, vacuum-based high temperature methods are often used to obtain highly crystalline ZnO films. However, these ZnO growth methods require sophisticated and expensive equipment and are unfeasible for the large scale fabrication of hybrid devices; hence, alternative solution-based methods which can be carried out at lower temperatures and are more economically viable and environmentally friendly are of great interest. Furthermore, solution processing of ZnO on organic films would allow greater flexibility in the choice of materials and architectures that could be used to construct hybrid electronic and photonic devices.

Preparation of ZnO nanostructures on organic substrates by electrodeposition from aqueous solutions offers several potential advantages over other solution-based techniques. Providing the organic substrate is conducting, electrodeposition is a simple, low-cost process which allows precise control over film thickness and morphology and can be easily applied on a large scale by modifying existing industrial electroplating procedures. Most importantly, highly crystalline ZnO films can, in principle, be electrodeposited at relatively low temperatures (<90 °C) without the need for thermal annealing[17] which is essential for ensuring the stability of the underlying organic films. However,

Received: March 16, 2011
Revised: May 25, 2011
Published: August 04, 2011

ACS Publications © 2011 American Chemical Society

performing electrochemistry on organic semiconductors is not trivial because of the relatively poor conductivity and electrochemical activity of these materials in aqueous solutions and therefore, the challenge is to develop a method for homogeneous growth of ZnO over the entire organic surface.

Only a few reports have been published very recently regarding the deposition of ZnO onto organic films. Luka et al.[18] reported the fabrication of *p-n* junction diodes by depositing ZnO onto pentacene thin films using atomic layer deposition, while Bano et al.[6] used chemical deposition methods to deposit ZnO nanorods onto polymeric flexible plastic substrates to fabricate white light emitting diodes. In addition, Lee et al.[19] electrochemically deposited ZnO nanostructures onto polypyrrole films to demonstrate that the synthetic method used to prepare the electrodes could provide inexpensive and sufficiently conductive supports to realize large-scale preparation of ZnO nanostructures for device applications; however, it is noted that these authors did not characterize the chemical purity of the electrodeposited ZnO films, and films deposited from electrolyte solutions containing high concentrations of $Zn(NO_3)_2$ (>20 mM) and 0.1 M KCl have been shown by other workers to contain zinc hydroxychloride compounds.[20,21] Furthermore, the low conductivity and inhomogeneous surface reactivity of the polypyrrole films made homogeneous deposition of ZnO over the entire surface area difficult to achieve. The use of a seed-layer assisted electrochemical approach reported by Hsieh et al.[22] and Zhang et al.[5,23] resulted in the deposition of homogeneous ZnO nanorod arrays on transparent and conductive polymeric and reduced graphene oxide films, respectively. The ZnO seeds provide nucleation sites for further ZnO growth. On thin reduced graphene oxide electrodes (11 nm thick) homogeneous and dense arrays of ZnO nanorods were grown over the entire surface; however, large pores were observed in the nanorod film deposited on flexible polyethylene napthalate substrates because of inhomogeneous surface reactivity. In general, reports of ZnO deposition onto organic films have been mainly focused toward device preparation and characterization. To our knowledge, studies of the growth mechanisms for the deposition of ZnO nanostructures onto organic substrates have not yet been reported.

In this paper, we describe the use of a two-step electrochemical process to homogeneously deposit ZnO nanostructured arrays *directly* onto organic-semiconducting substrates comprising copper phthalocyanine (CuPc) and pentacene thin films. To our knowledge, this is the first time the electrochemical deposition of ZnO onto molecular thin films has been reported. The π-conjugated small molecule materials used in this study were chosen to demonstrate that the electrodeposition of ZnO is not specific to a particular organic system and because these materials are used extensively for integration into a flexible range of electronic devices. For example, the strong photon absorption properties of CuPc make it attractive for use in solar cells[3] and photodiodes,[12] while ZnO-pentacene hybrid films are being developed as *p-n* junction diodes[24] and for field-effect transistors.[25] In our work, cyclic polarization studies reveal that the mechanism for ZnO deposition via the electroreduction of hydroxide precursor species (oxygen and NO_3^- ions) at π-conjugated organic thin films is analogous to that previously reported for conventional inorganic and metal electrodes. For the electrodeposition of highly uniform and homogeneously distributed arrays of nanostructured ZnO films on organic electrodes, two essential activation processes were identified: (1) electrochemical activation of the organic films toward NO_3^- reduction; and (2) activation of the electrode surface by deposition of a thin layer of ZnO nanoparticles, which subsequently act as nuclei for further ZnO film growth. In the two-step electrodeposition process, the surface is activated during the first step by applying a high cathodic overpotential. This is followed by film growth at lower overpotentials during the second electrolysis step.

2. EXPERIMENTAL SECTION

2.1. Materials and Reagents. Zinc nitrate hexahydrate ($Zn(NO_3)_2 \cdot 6H_2O$, Aldrich, 99%), potassium chloride (KCl, BDH Chemicals Ltd.), copper(II) phthalocyanine (CuPc, Aldrich, 97%), and pentacene (Kintec, sublimation grade) were used as received. Aqueous solutions were prepared using deionized (DI) water (>18 MΩ cm, Ondeo Purite), and oxygen and argon gases were supplied by BOC Gases Ltd.

2.2. Preparation of CuPc and Pentacene Films. CuPc and pentacene films with nominal thicknesses of 100 nm were deposited on ITO-coated glass substrates (PsiOTec Ltd., 15 Ω/sq.) by thermal evaporation at a base pressure of 10^{-7} mbar using a Kurt J. Lesker deposition chamber. Prior to film growth, the ITO substrates were ultrasonicated in successive baths of toluene, acetone, methanol, and isopropanol for 15 min each followed by rinsing with a stream of isopropanol and then dried with compressed air. CuPc and pentacene were evaporated from Knudsen cells at 420 and 190 °C, respectively, corresponding to a nominal growth rate of 1 Å s^{-1}, on the ITO substrates at room temperature. The thickness of the films was monitored in situ using calibrated quartz crystal microbalances situated near the substrates. After thermal evaporation, the CuPc/ITO and pentacene/ITO substrates were stored under vacuum until use. Ex situ characterization of the film thickness was performed by scanning electron microscopy (SEM).

2.3. Electrochemistry and Surface Characterization. Electrochemical measurements were carried out using a computer-controlled Eco Chemie Autolab PGSTAT 302 potentiostat and a conventional three-electrode cell setup consisting of a CuPc/ITO or pentacene/ITO working electrode (1.44 cm^2), a platinum mesh counter electrode, and a Ag/AgCl (saturated with KCl) reference electrode. The pentacene/ITO substrates were used as prepared; however, the CuPc/ITO substrates were thermally annealed in air at 150 °C for 1 h prior to use to improve adhesion. Electrochemical characterization of the organic layers was performed in Zn-free and Zn-containing electrolytes at 80 °C, bubbled with oxygen or argon gas (to deaerate the solution), using the cyclic polarization technique. Subsequent electrochemical deposition was performed in potentiostatic mode. The electrodeposition of ZnO was carried out at 80 °C in aqueous $Zn(NO_3)_2$ solutions (5 mM), containing 0.1 M KCl as the supporting electrolyte (total cell volume was 400 mL). The deposition bath was saturated with oxygen by bubbling oxygen gas through the solution vigorously for 30 min prior to carrying out any electrochemical measurements, and a gentle flow of $O_{2(g)}$ was maintained during deposition. A two-step electrolysis method was employed whereby a seed-layer was first deposited on the organic substrate by applying potentials more negative than that typically required for deposition of ZnO. In this work, seed-layers were deposited on to pentacene and CuPc thin films by applying −1.35 V for 10 and 15 s, respectively. For subsequent ZnO film growth, the deposition potential was maintained for 30 min at −0.80 V for CuPc and −0.90 V for pentacene coated electrodes. The deposition potentials used in this work were chosen to maximize the surface coverage and homogeneity of the nanostructured ZnO films. After deposition, the samples were rinsed with DI water and dried under a stream of compressed air. The morphologies of the ZnO seed-layers and films were characterized using a LEO Gemini 1525 Field Emission Gun SEM (FEGSEM) with an accelerating voltage of 5 keV. X-ray diffraction (XRD) patterns were recorded to identify the crystalline structure and orientation of the CuPc, pentacene and ZnO films using a Philips PANalytical X'Pert PRO MPD

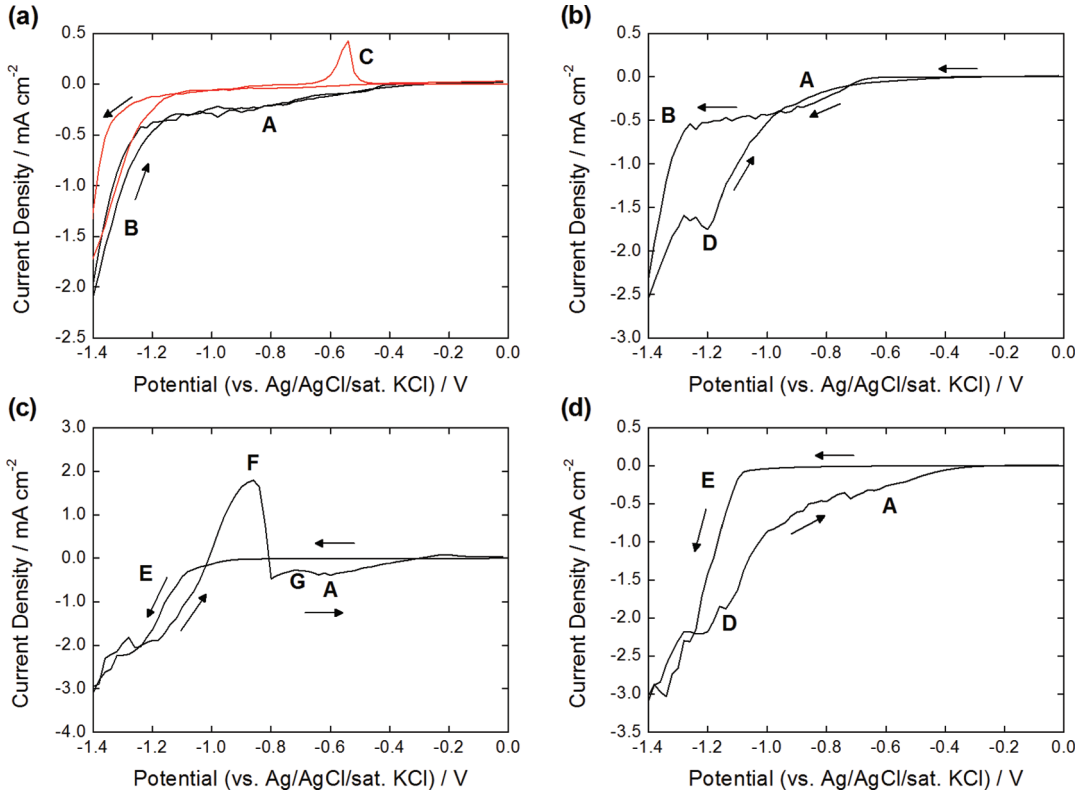

Figure 1. Cyclic polarization curves recorded at CuPc/ITO of: (a) 0.1 M KCl saturated with $O_{2(g)}$ (black solid lines) and $Ar_{(g)}$ (red solid lines); (b) 0.1 M KNO_3, (c) 5 mM $ZnCl_2$, and (d) 5 mM $Zn(NO_3)_2$ saturated with $O_{2(g)}$. For scans (c) and (d) the supporting electrolyte was 0.1 M KCl. All voltammograms were recorded at a solution temperature of 80 °C and a scan rate (υ) of 10 mV s^{-1}. Labels A−F refer to the following electrochemical reactions: (A) oxygen reduction; (B) hydrogen evolution and formation of surface-bound metallic tin; (C) reoxidation of surface-bound metallic tin; (D) nitrate reduction; (E) deposition of metallic zinc; (F) formation of ZnO, and (G) oxidation of surface-bound Zn−Sn alloys.

diffractometer with Cu Kα radiation and a Ni filter operated at 40 kV and 40 mA.

3. RESULTS AND DISCUSSION

3.1. Cyclic Polarization Studies of ZnO Electrodeposition onto CuPc and Pentacene Thin Films. The mechanism of ZnO deposition by electrochemical methods has been widely studied at conventional inorganic and metal electrodes.[26−31] This process is based on the electroreduction of dissolved oxygen and/or NO_3^- ions to generate OH^- ions (eqs 1 and 2) which increase the interfacial pH at the electrode surface leading to the precipitation of ZnO when Zn^{2+} ions are present in solution (eq 3).

$$NO_3^- + H_2O + 2e^- \rightarrow NO_2^- + 2OH^- \quad (1)$$

$$\frac{1}{2}O_2 + H_2O + 2e^- \rightarrow 2OH^- \quad (2)$$

$$Zn^{2+} + 2OH^- \rightarrow Zn(OH)_2 \rightarrow ZnO + H_2O \quad (3)$$

To understand the electrochemical behavior of semiconducting molecular thin films for ZnO deposition, survey experiments were initially carried out at CuPc/ITO electrodes using the cyclic polarization technique to study oxygen and nitrate reduction in the absence and presence of zinc (Figure 1). When only oxygen is present in 0.1 M KCl solution, a broad cathodic wave is observed between −0.40 and −1.25 V (Figure 1a, A) corresponding to the reduction of oxygen as shown in eq 2. The sharp increase in cathodic current at more negative potentials is attributed to the onset of hydrogen evolution by comparison with the cyclic polarization curve recorded in the absence of oxygen (Figure 1a, B). In addition, a brown color-change at the electrodes is also observed upon scanning to −1.40 V in deaerated and oxygenated 0.1 M KCl solutions. This occurs as a result of the reduction of tin oxide present in the ITO to metallic tin[26] and is associated with the peak observed at −0.55 V in the anodic scan of the cyclic polarization curve recorded in the deaerated solution, which corresponds to *reoxidation* of surface-bound metallic tin (Figure 1a, C). In comparison, the oxidation of metallic tin is not observed in the anodic scan when oxygen is present in solution because the corresponding peak is masked by the cathodic current of oxygen reduction between −1.25 and −0.40 V (Figure 1a, A).

When NO_3^- ions are introduced into solution, only the electroreduction of oxygen is observed in the first cathodic scan and the onset of this reaction is shifted to −0.60 V (Figure 1b, A); however, scanning the CuPc/ITO electrode to a lower potential limit of −1.40 V appears to electrochemically activate the organic layer as greater currents are measured in the anodic scan and a cathodic peak corresponding to nitrate reduction is now observed at −1.20 V (Figure 1b, D). Electrocatalytic activity of CuPc for the electroreduction of nitrate in alkaline media has been previously reported;[32] however, the authors did not comment on the origin of the induced catalytic activity. A possible explanation for this effect could be that oxygen adsorption on the organic surface from the deposition solution increases the surface conductivity.[33−36]

dx.doi.org/10.1021/cm200764h |*Chem. Mater.* 2011, 23, 3863–3870

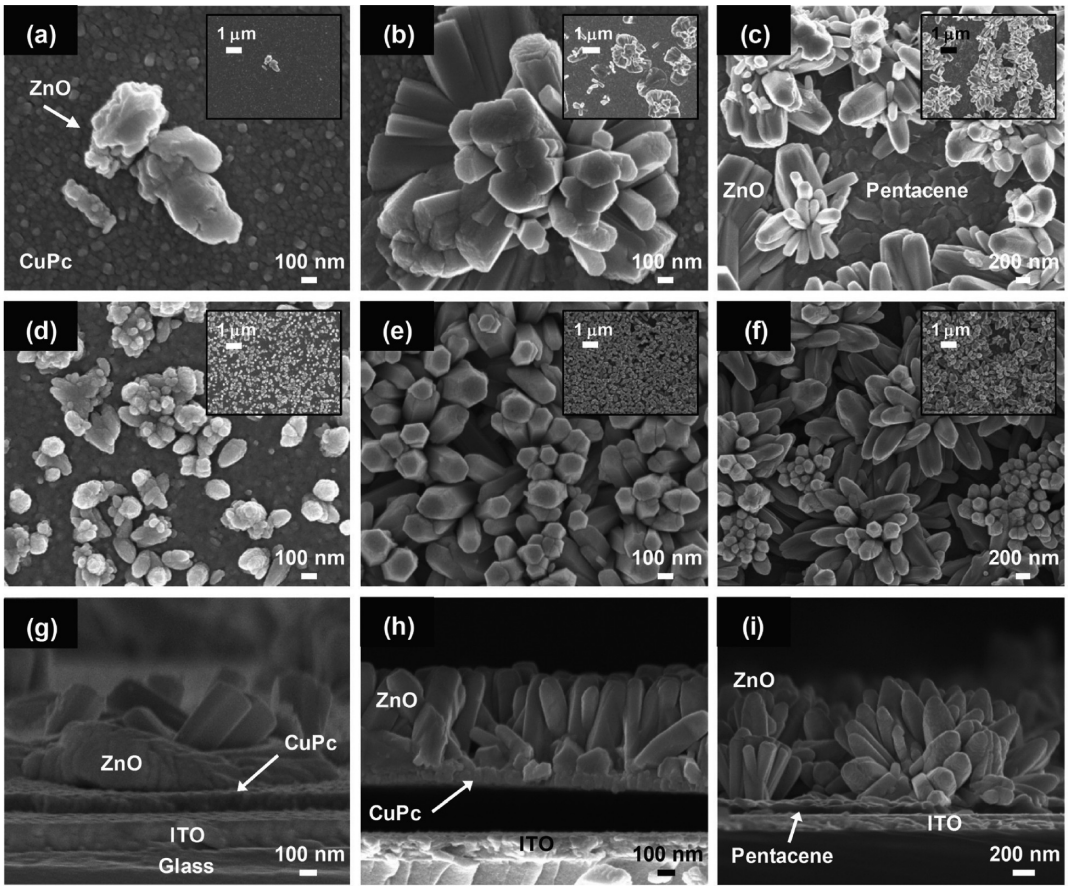

Figure 2. FEGSEM images of ZnO growth on CuPc (a, b, d, e, g, h) and pentacene (c, f, i) substrates from 5 mM $Zn(NO_3)_2$ solution containing 0.1 M KCl and saturated with $O_{2(g)}$ at 80 °C: Top-view images of (a) ZnO nucleation at −0.80 V after 15 s, (b) ZnO film growth at −0.80 V for 30 min, (c) ZnO film growth at −0.90 V for 30 min, (d) ZnO nucleation at −1.35 V for 15 s, (e) ZnO film growth onto seed-layer shown in (b) at −0.80 V for 30 min, and (f) ZnO film growth at −0.90 V for 30 min onto seed-layer deposited at −1.35 V for 10 s; (g−i) cross-sectional view images of (b), (e), and (f), respectively. Insets in (a−f) present low magnification images of the seed-layers and ZnO nanostructures.

Figures 1c−d show the cyclic polarization curves obtained at CuPc/ITO electrodes in oxygenated 5 mM $ZnCl_2$ and $Zn(NO)_3$ solutions containing 0.1 M KCl supporting electrolyte. When Zn^{2+} ions are present in solution, the expected oxygen reduction wave is not observed. A similar effect was observed by Canava et al. for the electroreduction of oxygen in $ZnCl_2$ solutions at tin oxide electrodes.[26] These authors attributed this effect to the adsorption of Zn-containing species on the electrode surface which consequently blocks the transfer of electrons to oxygen. From −1.10 to −1.40 V, the cathodic current increases sharply leading to the deposition of metallic zinc on the electrode surface (Figures 1c−d, E) which is subsequently oxidized to form ZnO when the polarization curve is reversed and scanned toward less negative potentials.[30] This oxidation process is clearly observed in $ZnCl_2$ solution as evidenced by the large anodic peak from −1.02 to −0.80 V (Figure 1c, F); however, in $Zn(NO_3)_2$ solutions the oxidation peak is masked because of the enhanced electrocatalytic activity of the CuPc surface for nitrate reduction (Figure 1d, D). The presence of Zn^{2+} ions has also been shown to catalyze nitrate reduction.[31] Furthermore, the ZnO layer deposited on the electrode surface as a result of the zinc reduction and oxidation process is observed to activate oxygen reduction in the reverse scan as the current becomes more cathodic at potentials positive of −0.80 V (Figures 1c−d, A). This is consistent with previous reports of the mechanism of ZnO electrodeposition at tin oxide[26] and gold electrodes.[30] The oxidative current superimposed on the oxygen reduction current at −0.71 V in the anodic scan of Figure 1c (G) is attributed to the reoxidation of Zn−Sn alloys formed on the surface.

From this cyclic polarization study, the potential window for ZnO deposition onto CuPc thin films is determined to be between −0.40 and −1.10 V. Similar behavior is observed using pentacene/ITO electrodes (see Supporting Information); hence, the mechanism of ZnO electrodeposition is assumed to be the same at the surface of both CuPc and pentacene thin films with electron transfer being dominated by the conjugated π-system present in these organic molecules and only marginally involving, if not at all, the central metal cation in the CuPc.

3.2. Effect of Seed-Layer Assisted Electrodeposition of ZnO Films onto CuPc and Pentacene Thin Films. Electrochemical activation of the CuPc and pentacene films for nitrate and oxygen reduction prior to ZnO film growth is *vital* for depositing a dense array of ordered nanostructures onto the organic-semiconducting substrates. The influence of potentiostatic pretreatment conditions on the nucleation and morphology of ZnO films electrodeposited on CuPc and pentacene layers from oxygenated 5 mM $Zn(NO_3)_2$ solution containing 0.1 M KCl supporting electrolyte is shown in the series of FEGSEM images in Figure 2.

For ZnO deposited by one-step electrolysis at applied potentials of −0.80 and −0.90 V for CuPc and pentacene coated

dx.doi.org/10.1021/cm200764h |*Chem. Mater.* 2011, 23, 3863–3870

electrodes, respectively, only a few particles form on the surface during the initial nucleation stages, separated by large areas of bare substrate (Figure 2a). This low nucleation density occurs because at these applied potentials the molecular films have not been electrochemically activated and the electroreduction of oxygen and NO_3^- ions is kinetically slow. After 30 min deposition time, the resulting ZnO films consist of aggregates of ZnO nanorods which have a broad distribution of rod diameters and are inhomogeneously distributed over the surface (Figure 2b, c and g). It is also noted that delamination of the CuPc films from the ITO substrates occurs under these conditions from areas where no ZnO is deposited.

In comparison, the use of a two-step electrolysis method to pretreat the CuPc and pentacene films at −1.35 V for 15 and 10 s, respectively, prior to ZnO film growth, electrochemically activates the molecular thin films for nitrate and oxygen reduction (see Section 3.1). A high density of particles (typically 100 nm in size) is deposited homogeneously over the organic surface and provides a seed-layer for subsequent film growth (Figure 2d). The density of the particle layer increases as the applied potential is shifted more negative; however, in this work, potentials more negative than −1.40 V were not investigated to avoid reducing Sn^{2+} ions present in the ITO substrate to metallic tin which affects the transparency of the electrode. At the potential of −1.35 V used for the first electrolysis step, the particle layer is most likely composed of metallic zinc which is then oxidized to ZnO post formation. In the two-step process, the metallic zinc deposited during nucleation will be oxidized to ZnO during the second electrolysis step when the applied potential is switched to −0.80 or −0.90 V for film growth on CuPc and pentacene substrates, respectively. The top-view and cross-sectional FEG-SEM images shown in Figures 2e−f and 2h−i for ZnO films grown via seed-layer assisted electrodeposition on CuPc and pentacene substrates, respectively, reveal that the films consist of uniform and dense arrays of ZnO nanorods with a narrow size distribution. The average film thickness of ZnO electrodeposited onto CuPc and pentacene substrates is approximately 0.60 and 1.0 μm, respectively, although the actual thickness is difficult to quantify because of the nanostructured nature of the deposits (see Figure 2). Importantly, the ZnO nanostructures deposited by the two-step deposition method are homogenously distributed over the entire surface of the organic substrates and no delamination occurs. Furthermore, the cross-sectional FEG-SEM (Figure 2h−i) and TEM images (not shown) confirm that there are no pinholes in the molecular thin films and that these films are stable and remain intact during the electrodeposition of ZnO *directly* onto the surface of the organic substrate.

Figure 3 presents XRD data obtained for ZnO films deposited by one- and two-step electrolysis onto CuPc and pentacene substrates. The peaks indicated by stars correspond to the ITO supporting substrate. All other diffraction peaks are assigned to CuPc, pentacene and hexagonal wurtzite ZnO (JCPDS No. 01-080-0074). Highly textured (100) and (001) out-of-plane orientations are observed for the CuPc and pentacene films, respectively. In comparison, the ZnO films electrodeposited by one or two-step electrolysis onto the organic substrates all show multi-directional growth indicating that they are polycrystalline. Preferential orientation of the ZnO films was estimated by calculating the texture coefficients (TC) using eq 4:[37]

$$TC(hkl) = \frac{I(hkl)}{I_0(hkl)} \Big/ \frac{1}{n}\sum \frac{I(hkl)}{I_0(hkl)} \qquad (4)$$

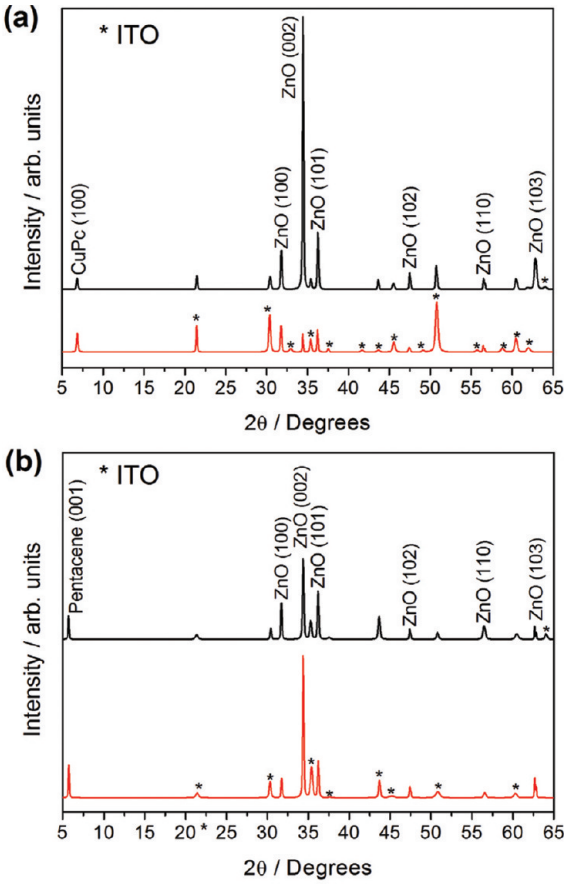

Figure 3. X-ray diffraction patterns of ZnO films electrodeposited onto (a) CuPc and (b) pentacene thin films by one-step (red solid lines) and two-step electrolysis (black solid lines) from 5 mM $Zn(NO_3)_2$ solution containing 0.1 M KCl and saturated with $O_{2(g)}$ at 80 °C. One-step electrolysis was carried out at (a) −0.80 V and (b) −0.90 V. For two-step electrolysis, the applied potentials were switched from (a) −1.35 → −0.80 V and (b) −1.35 → −0.90 V. Peaks labeled with an asterisk correspond to the ITO substrate.

where $TC(hkl)$ is defined as the texture coefficient of a specific (hkl) plane, $I(hkl)$ is the measured relative intensity, $I_0(hkl)$ is the relative intensity of the corresponding plane given in the JCPDS data, and n is the total number of reflections considered (Note: all the ZnO reflections labeled in the XRD patterns shown in Figure 3 were taken into account for this calculation). According to eq 4, the ZnO films will present preferential orientation if the TC for a specific (hkl) plane is greater than unity. The TC for the three main ZnO reflections ((100), (002), and (101)) present in the XRD patterns of the ZnO films deposited onto CuPc and pentacene substrates are given in Table 1. ZnO films deposited onto CuPc by one-step electrolysis without a seed-layer exhibit random crystallite orientation; however, when seed-layer assisted deposition of ZnO is performed using the two-step electrolysis method, a well-defined preferred orientation in the polar [002] direction is imparted into the film indicating that the *c*-axis is orientated perpendicular to the organic substrate. This result agrees well with the morphology of the film characterized by FEGSEM in Figure 2h which shows rod structures orientated perpendicular to the substrate. In comparison, the (002) preferential orientation is observed for ZnO films deposited onto pentacene layers by both one- and two-step electrolysis, but this

Table 1. Effect of ZnO Particle Seed-Layer on the Texture and Crystallite Domain Size of ZnO Films Electrodeposited onto CuPc and Pentacene Thin Film Substrates

		CuPc		pentacene	
	ZnO reflection (*hkl*)	without seed-layer	with seed-layer	without seed-layer	with seed-layer
texture coefficient	100	1.50	0.33	0.37	0.87
	002	1.55	4.12	3.70	2.41
	101	0.83	0.29	0.36	0.64
crystallite domain size (nm)	100	47.96	42.06	42.05	48.37
	002	46.19	41.21	46.77	46.78
	101	40.31	36.05	40.57	40.59

is less significant compared to seed-layer assisted ZnO growth on CuPc substrates. Compared to CuPc, an increase in growth in the nonpolar [100] and [101] directions is seen on pentacene substrates (see Table 1) which is consistent with the flower-like morphology observed for these films in Figures 2c and f. Furthermore, the preferential orientation of ZnO films electrodeposited on pentacene substrates is observed to decrease to a greater extent when growth is carried out on top of a ZnO seed-layer by two-step electrolysis. This effect is attributed to misorientation of the rods with respect to the substrate rather than a change in the crystallinity of the rods themselves (see Figure 2i).

Figure 4 shows the cathodic current density-time curves measured for ZnO film growth on CuPc and pentacene substrates without (one-step electrolysis) and with seed-layers (two-step electrolysis). Correlation of the cathodic current density-time curves with film morphology and orientation shows that ZnO film growth on organic substrates is dependent on (1) cathodic current density (and hence, local pH at the electrode surface); and (2) the number of nucleation sites. The cathodic current passed during deposition corresponds to the reduction of oxygen and NO_3^- ions (eqs 1 and 2); therefore, the higher the cathodic current density, the greater the increase in local pH at the electrode surface, which leads to increased deposition of ZnO. This occurs because the current density is below the diffusion limit of Zn^{2+} ions.[38] For example, the low cathodic current density observed for ZnO film growth on CuPc in the absence of a seed-layer (Figure 4a, scan i) corresponds to an insufficient increase in interfacial pH at the electrode surface and results in the precipitation of a low density of nucleation sites (see Figure 2a), where randomly orientated ZnO crystals slowly grow larger with deposition time (see Figures 2b, g and 3a). In contrast, when ZnO films are grown on top of a preformed ZnO seed-layer deposited on the CuPc surface, the cathodic current density is significantly increased (Figure 4a, scan ii) because the seeds provide a high density of sites which activate the surface for the electroreduction of oxygen and NO_3^- ions. Under these conditions, the deposition rate of ZnO is increased with growth occurring directly on the already formed nuclei along the wurtzite *c*-axis (Figure 2h and 3a). By comparison, it is noted that the cathodic current densities recorded for ZnO films grown on pentacene substrates in the absence and presence of a ZnO seed-layer (Figure 4b, scans i and ii) are very similar to that measured for seed-layer assisted film growth on CuPc substrates (Figure 4a, scan ii), and all these films exhibit preferred orientation in the [002] direction (Figure 3). Therefore, the orientation of ZnO films electrodeposited on organic substrates can be controlled by adjusting the cathodic current density. This result is analogous

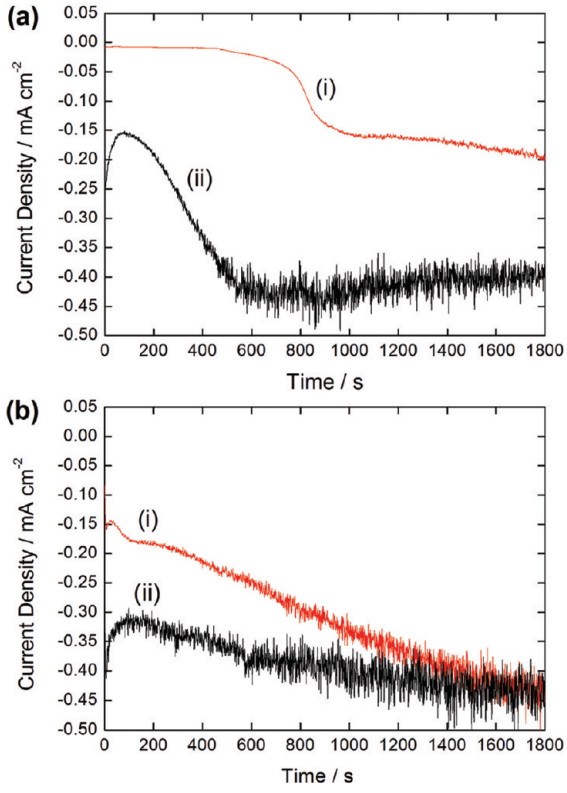

Figure 4. Cathodic current density-time curves for ZnO film growth on (a) CuPc and (b) pentacene thin films in the (i) absence and (ii) presence of a ZnO seed-layer. The deposition solution was 5 mM $Zn(NO_3)_2$ at 80 °C, containing 0.1 M KCl supporting electrolyte and saturated with $O_{2(g)}$. The applied potentials for ZnO film growth were (a) −0.80 V and (b) −0.90 V.

to the findings of Izaki et al.[39] and Mahalingam et al.[40] who independently reported that the orientation of ZnO films electrodeposited onto tin oxide electrodes is dependent on cathodic current density. The difference in cathodic current density measured for one-step electrolysis of ZnO on CuPc and pentacene substrates (compare Figures 4a and 4b, scan i) may be related to increased conductivity and/or redox activity of pentacene compared to CuPc.

The crystallite domain sizes of the CuPc, pentacene and ZnO films were estimated using the Scherrer equation[41] based on the full-width half-maximum (fwhm) data extracted from Figure 3. No significant changes in the orientation and crystallite domain size of the CuPc ((100)-orientated crystallites, 48 nm) and

pentacene films ((001)-orientated crystallites, 60 nm) are observed after ZnO electrodeposition confirming that the structural integrity of the molecular thin films is retained during electrochemical treatment. The domain size of the primary ZnO crystallites are given in Table 1 for films deposited onto CuPc and pentacene substrates without and with seed-layers. The calculated crystallite domain sizes are smaller than the average rod diameter (Figure 2) indicating that the individual structures are polycrystalline. Deposition of a ZnO seed-layer prior to film growth does not appear to significantly affect ZnO crystallite domain size. In addition, the ZnO crystallite domain sizes are very similar for films deposited onto CuPc and pentacene substrates. These results provide further evidence that electron transfer is dominated by the conjugated π-system of the CuPc and pentacene molecules.

4. CONCLUSIONS

The deposition of highly crystalline ZnO films *directly* onto semiconducting molecular thin films of CuPc and pentacene using low-temperature electrochemical methods has been successfully demonstrated for the first time. Cyclic polarization studies and XRD analysis reveal that the mechanism for ZnO electrodeposition by reduction of hydroxide precursor species is analogous to that previously reported for conventional inorganic and metal electrodes and that electron transfer across the organic thin films occurs via the conjugated π-system present in both organic molecules. To obtain uniform and dense arrays of ZnO nanostructures distributed homogeneously over the substrate surfaces, electrochemical activation of the molecular thin films by applying high overpotentials prior to film growth is *essential* to provide a high density of nucleation centers on which further ZnO growth can take place. A critical finding of this study is that the organic films are not degraded during electrodeposition and the film properties are preserved. The ability to process nanostructured inorganic ZnO films on top of organic layers using low-temperature, low-cost, and readily scalable electrochemical methods is envisaged to have important applications in the fabrication of a wide range of hybrid electronic devices such as sensors, light emitting diodes, solar cells, and display devices.

■ ASSOCIATED CONTENT

Supporting Information. Cyclic polarization curves recorded at pentacene/ITO electrodes in Zn-free and Zn-containing electrolytes (PDF). This material is available free of charge via the Internet at http://pubs.acs.org.

■ AUTHOR INFORMATION

Corresponding Author
*E-mail: m.p.ryan@imperial.ac.uk.

■ ACKNOWLEDGMENT

We gratefully acknowledge the U.K. Engineering and Physical Sciences Research Council (EPSRC) for financial support through a Nanotechnology Grand Challenge: Energy grant (EP/F056362/1 and EP/F056184/1). Assistance from Salahud Din and Jennifer Nekuda Malik regarding the growth of CuPc and pentacene films by thermal evaporation is also thankfully acknowledged.

■ REFERENCES

(1) Kumar, S. A.; Cheng, H. W.; Chen, S. M. *React. Funct. Polym.* **2009**, *69*, 364.
(2) Peiro, A. M.; Ravirajan, P.; Govender, K.; Boyle, D. S.; O'Brien, P.; Bradley, D. D. C.; Nelson, J.; Durrant, J. R. *J. Mater. Chem.* **2006**, *16*, 2088.
(3) Sharma, G. D.; Kumar, R.; Sharma, S. K.; Roy, M. S. *Sol. Energy Mater. Sol. Cells* **2006**, *90*, 933.
(4) Yoshida, T.; Zhang, J. B.; Komatsu, D.; Sawatani, S.; Minoura, H.; Pauporte, T.; Lincot, D.; Oekermann, T.; Schlettwein, D.; Tada, H.; Wohrle, D.; Funabiki, K.; Matsui, M.; Miura, H.; Yanagi, H. *Adv. Funct. Mater.* **2009**, *19*, 17.
(5) Yin, Z. Y.; Wu, S. X.; Zhou, X. Z.; Huang, X.; Zhang, Q. C.; Boey, F.; Zhang, H. *Small* **2010**, *6*, 307.
(6) Bano, N.; Zaman, S.; Zainelabdin, A.; Hussain, S.; Hussain, I.; Nur, O.; Willander, M. *J. Appl. Phys.* **2010**, 108.
(7) Konenkamp, R.; Word, R. C.; Godinez, M. *Nano Lett.* **2005**, *5*, 2005.
(8) Nadarajah, A.; Word, R. C.; Meiss, J.; Konenkamp, R. *Nano Lett.* **2008**, *8*, 534.
(9) Liu, J. P.; Wang, S. S.; Bian, Z. Q.; Shan, M.; Huang, C. H. *Appl. Phys. Lett.* **2009**, *94*, 173107.
(10) Sofos, M.; Goldberger, J.; Stone, D. A.; Allen, J. E.; Ma, Q.; Herman, D. J.; Tsai, W. W.; Lauhon, L. J.; Stupp, S. I. *Nat. Mater.* **2009**, *8*, 68.
(11) Chen, Y. F.; Bagnall, D. M.; Zhu, Z. Q.; Sekiuchi, T.; Park, K. T.; Hiraga, K.; Yao, T.; Koyama, S.; Shen, M. Y.; Goto, T. *J. Cryst. Growth* **1997**, *181*, 165.
(12) Karan, S.; Mallik, B. *Nanotechnology* **2008**, *19*, 495202.
(13) Choopun, S.; Vispute, R. D.; Noch, W.; Balsamo, A.; Sharma, R. P.; Venkatesan, T.; Iliadis, A.; Look, D. C. *Appl. Phys. Lett.* **1999**, *75*, 3947.
(14) Shinagawa, T.; Murase, K.; Otomo, S.; Katayama, J.; Izaki, M. *J. Electrochem. Soc.* **2009**, *156*, H320.
(15) Izaki, M.; Omi, T. *Appl. Phys. Lett.* **1996**, *68*, 2439.
(16) Peulon, S.; Lincot, D. *Adv. Mater.* **1996**, *8*, 166.
(17) Goux, A.; Pauporte, T.; Chivot, J.; Lincot, D. *Electrochim. Acta* **2005**, *50*, 2239.
(18) Luka, G.; Krajewski, T.; Wachnicki, L.; Szczepanik, A.; Fidelus, J. D.; Szczerbakow, A.; Lusakowska, E.; Kopalko, K.; Guziewicz, E.; Godlewski, M. *Acta Phys. Pol., A* **2008**, *114*, 1229.
(19) Lee, D. U.; Pradhan, D.; Mouawia, R.; Oh, D. H.; Heinig, N. F.; Leung, K. T.; Prouzet, E. *Chem. Mater.* **2010**, *22*, 218.
(20) Illy, B. N.; Ingham, B.; Ryan, M. P. *Cryst. Growth Des.* **2010**, *10*, 1189.
(21) Wang, F.; Liu, R.; Pan, A.; Cao, L.; Cheng, K.; Xue, B.; Wang, G.; Meng, Q.; Li, J.; Li, Q.; Wang, Y.; Wang, T.; Zou, B. *Mater. Lett.* **2007**, *61*, 2000.
(22) Hsieh, C. T.; Lin, J. Y.; Yang, S. Y. *Phys. E* **2010**, *42*, 2319.
(23) Wu, S. X.; Yin, Z. Y.; He, Q. Y.; Huang, X. A.; Zhou, X. Z.; Zhang, H. *J. Phys. Chem. C* **2010**, *114*, 11816.
(24) Pal, B. N.; Sun, J.; Jung, B. J.; Choi, E.; Andreou, A. G.; Katz, H. E. *Adv. Mater.* **2008**, *20*, 1023.
(25) Pal, B. N.; Trottman, P.; Sun, J.; Katz, H. E. *Adv. Funct. Mater.* **2008**, *18*, 1832.
(26) Canava, B.; Lincot, D. *J. Appl. Electrochem.* **2000**, *30*, 711.
(27) Gao, X. D.; Peng, F.; Li, X. M.; Yu, W. D.; Qiu, J. J. *J. Mater. Sci.* **2007**, *42*, 9638.
(28) Inamdar, A. I.; Mujawar, S. H.; Sadale, S. B.; Sonavane, A. C.; Shelar, M. B.; Shinde, P. S.; Patil, P. S. *Sol. Energy Mater. Sol. Cells* **2007**, *91*, 864.
(29) Ingham, B.; Illy, B. N.; Ryan, M. P. *J. Phys. Chem. C* **2008**, *112*, 2820.
(30) Peulon, S.; Lincot, D. *J. Electrochem. Soc.* **1998**, *145*, 864.
(31) Yoshida, T.; Komatsu, D.; Shimokawa, N.; Minoura, H. *Thin Solid Films* **2004**, *451*, 166.
(32) Chebotareva, N.; Nyokong, T. *J. Appl. Electrochem.* **1997**, *27*, 975.
(33) Zhou, Q.; Gould, R. D. *Thin Solid Films* **1998**, *317*, 432.

(34) Zhivkov, I.; Spassova, E.; Dimov, D.; Danev, G. *Vacuum* **2004**, *76*, 237.
(35) Petrovic, A.; Bratina, G. *Appl. Phys. Lett.* **2009**, 94.
(36) Parisse, P.; Picozzi, S.; Passacantando, M.; Ottaviano, L. *Thin Solid Films* **2007**, *515*, 8316.
(37) Barrett, C. S.; Massalski, T. B. *Structure of Metals: Crystallographic Methods, Principles and Data*; 3rd rev. ed.; Pergamon Press Ltd.: Oxford, 1980;
(38) Pauporte, T.; Lincot, D. *J. Electroanal. Chem.* **2001**, *517*, 54.
(39) Izaki, M.; Omi, T. *J. Electrochem. Soc.* **1997**, *144*, 1949.
(40) Mahalingam, T.; John, V. S.; Sebastian, P. J. *Mater. Res. Bull.* **2003**, *38*, 269.
(41) Klug, H. P.; Alexander, L. E. *X-Ray Diffraction Procedures For Polycrystalline and Amorphous Materials*; John Wiley & Sons, Inc.: New York, 1954; p 491.